Mobile Robot Localization and Mapping using a Gaussian Sum Filter

Ngai Ming Kwok, Quang Phuc Ha, Shoudong Huang, Gamini Dissanayake, and Gu Fang

Abstract: A Gaussian sum filter (GSF) is proposed in this paper on simultaneous localization and mapping (SLAM) for mobile robot navigation. In particular, the SLAM problem is tackled here for cases when only bearing measurements are available. Within the stochastic mapping framework using an extended Kalman filter (EKF), a Gaussian probability density function (pdf) is assumed to describe the range-and-bearing sensor noise. In the case of a bearing-only sensor, a sum of weighted Gaussians is used to represent the non-Gaussian robot-landmark range uncertainty, resulting in a bank of EKFs for estimation of the robot and landmark locations. In our approach, the Gaussian parameters are designed on the basis of minimizing the representation error. The computational complexity of the GSF is reduced by applying the sequential probability ratio test (SPRT) to remove under-performing EKFs. Extensive experimental results are included to demonstrate the effectiveness and efficiency of the proposed techniques.

Keywords: Distribution approximation, Gaussian sum filter, mixture reduction, simultaneous localization and mapping.

1. INTRODUCTION

Mobile robots have been utilized to work for and with humans in an ever increasing pace. In addition to the motorized mobility, it is a fundamental requirement that a mobile robot should be able to know its position within its operating environment before any assigned task can be accomplished [1], for example; in space exploration, underwater navigation, warehouse and office deliveries. Furthermore, *a priori* knowledge of the environment may not always be available, such as in cases of search and rescue operations, otherwise a cost has to be invested in structuring the environment. Therefore, it is important that the robot is able to build a map of its operating area. In most situations, the mobile robot is equipped with internal sensors, e.g., wheel encoders, that provide information on the robot motion from which the robot location is inferred. However, internal sensors operate in an open loop without ex-ternal references tend to accumulate location errors over time. External sensors, e.g., laser scanner, sonar or camera, are therefore frequently mounted on the mobile robot to provide some kind of external references to landmarks for its localization. External sensors may provide measurements in the form of range-and-bearing or just range-only or bearing-only measurements. Consequently, the type of sensor used plays a crucial role in the performance of any estimator or filter designed to localize the robot and to build a map.

The pioneering work on SLAM was presented in [2] and introduced the concept of state estimation. A framework using the stochastic mapping was proposed in [3] to estimate the robot location, based on the Bayesian estimation theory. It was implemented via an extended Kalman filter (EKF) with the availability of a range-and-bearing sensor. The work reported in [4] derived the convergence properties for the SLAM problem, using an EKF and also assuming that range-and-bearing measurements were available. Specifically, the stochastic mapping approach implements an EKF subjected to the pre-requisite that the system is linearizable and, most importantly, that the estimation uncertainty can be described by a Gaussian probability density function (pdf) whose characteristic parameters are the mean and covari-ance. The EKF then propagates the mean and co-variance through filter iterations and provides an optimal estimate in the sense of minimum mean-square-error. When range-and-bearing measurements are provided, the *a priori* pdf of a landmark can be characterized by a Gaussian and the EKF can be applied directly.

Manuscript received December 16, 2005; revised December 6, 2006 and January 23, 2007; accepted March 8, 2007. Recommended by Editorial Board member Sooyong Lee under the direction of Editor Jae-Bok Song. This work is supported by the ARC Centre of Excellence programme, funded by the Australian Research Council (ARC) and the New South Wales State Government, and the Early Career Researcher Grant, University of Technology, Sydney.

Ngai Ming Kwok, Quang Phuc Ha, Shoudong Huang, Gamini Dissanayake are with the ARC Centre of Excellence for Autonomous Systems (CAS), Faculty of Engineering, University of Technology, Sydney, Australia (e-mails: {ngai.kwok, quang.ha, sdhuang, gdissa}@eng.uts.edu.au).

Gu Fang is with the School of Engineering, University of Western Sydney, Australia (e-mail: g.fang@uws.edu.au).

However, when only the bearing measurement is obtained, specially designed estima-tors must be employed due to the violation of the spatial Gaussian pdf assumption. This bearing-only SLAM problem is the focus of the work presented here.

It is anticipated that for bearing-only SLAM, some form of representation of a non-Gaussian pdf should be adopted or appropriate filters have to be employed. In [5], a particle filter (PF) [6] was used to estimate the range of a landmark to the robot in a target tracking application. However, quite often the PF is computationally expensive because the repre-sentation of the non-Gaussian pdf requires a large number of weighted samples. The PF is also liable to the pre-mature convergence or sample impoverish-ment problem where samples tend to concentrate on a small region of the solution space. Hence, the PF needs to be modified to counteract the sample impoverishment problem [7]. An approach that makes use of reduced particle representation and Kalman filtering was reported in [8]. The technique can be traced to the fundamental derivation of the Gaussian sum filter (GSF) as proposed in [9]. For this, an arbitrary pdf is represented by a weighted sum of Gaussians and the estimation is proved to comply of EKFs. The basic idea is to coordinate multiple filters, each operates in an appropriate solution domain, and the results are optimized via a weighted sum. This philosophy is also applied in the form of a mixture of expert systems [10]. A variation of the weighted sum principle also found many applications such as in radar tracking [11], vehicle tracking [12] and air traffic control [13]. These implementations present an interactive multi-model configuration where computational complexity can be reduced.

The bearing-only SLAM problem requires some special treatment as the system dimension is not constant and measurements are incomplete due to the lack of range information. Initially, before any landmark is observed, the system contains only the robot location and orientation. The system dimension increases when landmarks are observed and included in the estimator, thus, leads to the initialization problem. As range information is missing, the landmark location cannot be inferred directly from one bearing measurement. A delayed initialization strategy was implemented in [14], whereby land-marks were incorporated into the EKF after con-firming that the associated uncertainty has been described with sufficient accuracy by a Gaussian pdf. The uncertainty was firstly represented by using a large number of samples and tested by a goodness-of-fit metric using the Kullback divergence. However, the use of numerous samples would increase the computational load. Similar delayed strategy using an EKF was described in [15] where the use of samples was avoided but delays were still encountered. Recently, there has been some research on implementing an un-delayed strategy where land-marks are incorporated into the estimator when they were firstly observed. In our preliminary work [16], a GSF was used in SLAM with efficiency improved by the sequential probability ratio test (SPRT). The un-delayed strategy was also adopted in [17] with special treatment on the representation by Gaussians. In the work therein, the non-Gaussian pdf was represented by the geometrically distributed hypoth-esis as suggested in [18].

The implementation of a GSF is, in fact, a parallel running of multiple EKFs. The major drawback of the GSF is its multiplicative complexity as compared to a single EKF. This observation naturally demands for an efficient implementation by removing redun-dant EKFs that do not contribute significantly to the state estimate. In [19], the significance of individual EKFs were checked statistically for removal through a greedy algorithm. An approach based on cost func-tions was adopted in [20] to decide on the con-struction of the Gaussian sum. However, these methods rely on the supply of samples as training data which is not rationally justifiable in the SLAM context. For this, the work in [21], where distances between Gaussian mixtures were derived, may be promising in dealing with the construction of Gaussian sums.

In this work, a GSF will be applied in solving the SLAM problem for a mobile robot using bearing-only measurements. The contributions of this paper are twofold. First, the choice of the number of Gaussians and their parameters in the GSF will be elaborated. Insights will be given by formulating a relationship between the Gaussians and a specific approximation error probability. Secondly, an effi-cient method that overcome the computational complexity will be proposed here. The test and removal of redundant EKFs will be implemented on the basis of the SPRT to guarantee a predefined tolerable decision error with a finite number of tests required.

The rest of the paper is organized as follows. In Section 2, the SLAM problem is briefly reviewed within the stochastic mapping framework and the need for Gaussian representation is introduced. Section 3 will be devoted to the development of the GSF with considerations on landmark initialization constraints, choice of GSF parameters and strategies to reduce the computational complexity. In Section 4, results from experiments using a Pioneer mobile robot will be given to illustrate the effectiveness of the proposed approach. Finally, a conclusion is drawn in Section 5.

2. LOCALIZATION AND MAPPING

When a mobile robot is deployed in its operating

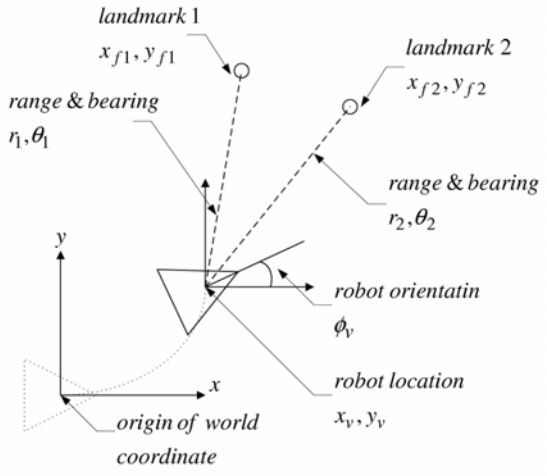

Fig. 1. Simultaneous localization and mapping.

environment, it is required that the robot keeps tracking of its own location and orientation, and be able to model the environment in the form of a feature based map. Fig. 1 illustrates the SLAM process for the conventional range-and-bearing case. This problem is cast as a state estimation process where the Bayesian estimation philosophy is applied.

The location of the robot is referred to a world-coordinate frame and its orientation is measured counterclockwise with respect to the x-axis. Landmarks are assumed to be scattered across the operating area and the sensor returns range and bearing measurements relatively to the robot position. The robot motion is described by a system or process model and the sensor is characterized by a measurement model.

2.1. System model

Let the system be described by a state vector and evolves in discrete time, that is [1]

$$\mathbf{x}_{k+1} = \mathbf{f}(\mathbf{x}_k, \mathbf{u}_k + \mathbf{w}_k), \tag{1}$$

where $\mathbf{x}$ is the state vector consisting of the robot and landmark locations, $\mathbf{f}$ is the process model, $\mathbf{u}$ is the control command, $\mathbf{w}$ is the control noise having a Gaussian pdf and subscript k is the discrete time index.

The state is, in general, not directly measurable but through noisy measurements described by a measurement model

$$\mathbf{z}_k = \mathbf{h}(\mathbf{x}_k) + \mathbf{v}_k, \tag{2}$$

where $\mathbf{h}$ is the observation function and $\mathbf{v}$ is the observation noise with an arbitrary statistical characteristic.

In the Bayesian estimation framework, informa-tion about the system is contained in the *a posterior* pdf. When observations are available, we are interested in the conditional pdf

$$p(\mathbf{x}_k \mid \mathbf{Z}_k) = \frac{p(\mathbf{z}_k \mid \mathbf{x}_k) p(\mathbf{x}_k \mid \mathbf{Z}_{k-1})}{p(\mathbf{z}_k \mid \mathbf{Z}_{k-1})}, \tag{3}$$

where $\mathbf{Z}_k$ is the aggregated observations available up to time k, and

$$p(\mathbf{z}_k \mid \mathbf{Z}_{k-1}) = \int p(\mathbf{z}_k \mid \mathbf{x}_k) p(\mathbf{x}_k \mid \mathbf{Z}_{k-1}) d\mathbf{x}_k, \tag{4}$$

is a normalization factor.

Further manipulation can lead to a recursive estimator given by a prediction step as

$$p(\mathbf{x}_k \mid \mathbf{Z}_{k-1}) = \int p(\mathbf{x}_k \mid \mathbf{x}_{k-1}) p(\mathbf{x}_{k-1} \mid \mathbf{Z}_{k-1}) d\mathbf{x}_{k-1}. \tag{5}$$

When implementing the above Bayesian estimation procedure for the special case of a linear process/observation system with noises described by a single Gaussian, the well known Kalman filter can be applied. For non-linear process/observation models, an EKF is frequently used, provided that the system is linearizable.

2.2. Stochastic mapping

When the discrete sampling time is small and the robot is moving at a low speed, the process model may be linearized by a Taylor series expansion from which the EKF is derived. Furthermore, if the sensor is able to provide sufficiently accurate measurement to landmarks (e.g., range-and-bearing measurements), then the observation model is also linearizable with acceptable linearization errors. In practice, most sensors can be characterized by a Gaussian pdf on its measurement errors. Based on the above conditions, the stochastic mapping for a mobile robot proceeds as given in the following steps with the use of an EKF [3].

1. When $k = 0$, set

$$\mathbf{x}_0 = \mathbf{x}_{v,0} \leftarrow 0^{3\times 1}, \tag{6a}$$

$$\mathbf{P}_0 = \mathbf{P}_{v,0} \leftarrow 0^{3\times 3}, \tag{6b}$$

where the subscript v stands for the robot, $\mathbf{x}_v = [x_v, y_v, \varphi_v]^T$, (x_v, y_v) is the robot location and φ_v is the robot orientation. The zero settings denote the initial location of the robot being at the origin of a co-ordinate frame with zero uncertainty.

2. When $k \geq 0$, issue command $\mathbf{u}_k$ to drive the robot and make prediction on the robot state, according to

$$\mathbf{x}_{k+1|k} = \mathbf{f}(\mathbf{x}_{k|k}, \mathbf{u}_k), \tag{7a}$$

$$\mathbf{P}_{k+1|k} = \nabla \mathbf{f}_x \mathbf{P}_{k|k} \nabla \mathbf{f}_x^T + \nabla \mathbf{f}_u \Omega \nabla \mathbf{f}_u^T, \tag{7b}$$

where the notation $(k+1|k)$ denotes the transition from time k to $k+1$, $\nabla \mathbf{f}_x$ and $\nabla \mathbf{f}_u$ are Jacobians of the process model with respect to the state and control, and Ω is the covariance matrix of the odometer noise given by

$$\Omega = \begin{bmatrix} \sigma_v^2 & 0 \\ 0 & \sigma_\gamma^2 \end{bmatrix}, \tag{8}$$

where σ_v and σ_γ are the standard deviations of the speed and turn-rate measurement noise.

3. If an observation, with range and bearing (r,θ) is declared from a new landmark, then perform the initialization as follows.
(a) Generate an initialization function

$$\mathbf{g} = (\mathbf{x}_v^T, \mathbf{x}_{fo}^T, \mathbf{x}_f^T(r,\theta))^T, \tag{9}$$

where $\mathbf{x}_{fo}$ is some previously registered landmark, $\mathbf{x}_f(r,\theta)$ is the newly observed landmark with the range and bearing measurements and

$$\mathbf{x}_f(r,\theta) = \begin{bmatrix} x_v + r\cos(\varphi_v + \theta) \\ y_v + r\sin(\varphi_v + \theta) \end{bmatrix}. \tag{10}$$

(b) Perform system augmentation

$$\mathbf{x}_{k+1|k} \leftarrow [\mathbf{x}_v^T, \mathbf{x}_{fo}^T, \mathbf{x}_f^T]^T, \tag{11a}$$

$$\mathbf{P}_{k+1|k} \leftarrow \nabla \mathbf{g} \mathbf{P}^- \nabla \mathbf{g}^T, \tag{11b}$$

where

$$\mathbf{P}^- = \begin{bmatrix} \mathbf{P}_{k+1|k} & 0 \\ 0 & \mathbf{R} \end{bmatrix}, \tag{12a}$$

$$\mathbf{R} = \begin{bmatrix} \sigma_r^2 & 0 \\ 0 & \sigma_\theta^2 \end{bmatrix}, \tag{12b}$$

σ_r, σ_θ are the standard deviations of the range and bearing measurement noise assuming a Gaussian pdf, and $\nabla \mathbf{g}$ is the Jacobian of the initialization function with respect to the system state and measurements.

4. If the observation is from a previously registered landmark through a data association process, then perform a Kalman filter update by calculating

$$\nu = \mathbf{z} - \mathbf{h}(\mathbf{x}_{k+1|k}), \tag{13a}$$

$$\mathbf{S} = \nabla \mathbf{h} \mathbf{P}_{k+1|k} \nabla \mathbf{h}^T + \mathbf{R}, \tag{13b}$$

$$\mathbf{K} = \mathbf{P}_{k+1|k} \nabla \mathbf{h}^T \mathbf{S}^{-1}, \tag{13c}$$

and

$$\mathbf{x}_{k+1|k+1} = \mathbf{x}_{k+1|k} + \mathbf{K}\nu, \tag{14a}$$

$$\mathbf{P}_{k+1|k+1} = \mathbf{P}_{k+1|k} - \mathbf{K}\mathbf{S}\mathbf{K}^\mathbf{T}, \tag{14b}$$

where ν is the innovation, $\mathbf{S}$ is the innovation covariance, $\nabla \mathbf{h}$ is the Jacobian of the measurement model with respect to the robot and measured landmark, $\mathbf{K}$ is the Kalman gain.

2.3. Bearing-only SLAM

Bearing-only SLAM is more challenging than the range-and-bearing SLAM process as the sensor only provides bearing measurements. As noted from the stochastic mapping procedures, it is difficult to initialize a landmark without range information. Furthermore, a Gaussian pdf is ineffective to describe the associated uncertainty in the range to the landmark. Some researchers have adopted a delayed initialization strategy, e.g., [14] and [15]. However, it is generally not straightforward to assign decision rules (with specific probability of error in decisions) and to determine when such decision can be made in order to incorporate a new landmark into the system. Fortunately, a further investigation into the stochastic mapping procedure reveals that, if the noise characteristic from the bearing measure can be modelled as a Gaussian then the EKF iterations can still be applied.

In the current research, we will present an application of the Gaussian sum filter consisting of a bank of EKFs to the bearing-only SLAM problem. This filter is a very attractive candidate as the EKFs can be applied with a proper representation of the initial pdf for the range to a landmark. The computational burden of using a bank of parallel EKFs will be resolved by reducing the number of EKFs through a hypothetical test where decision errors can be explicitly specified.

3. GAUSSIAN SUM FILTERING

The Gaussian sum filter is directed towards representing an arbitrary pdf with the use of a mixture or a number of weighted Gaussian pdfs. It has been demonstrated that the representation error can be maintained at a low level, with proper choices on the mixture parameters, namely, the set of weighting factors, the means and variances of the Gaussians. Fig. 2 illustrates the concept of a Gaussian sum filter. Each Gaussian is operative in an EKF which conducts its own estimation of the robot and landmark location. Their outputs are then weighted and summed to provide an overall aggregated estimation.

In general, for an arbitrary pdf, one can have the following approximate distribution.

$$p(\mathbf{x}) \approx \sum_{i=1}^{N} \alpha_i \mathbf{N}(\mathbf{m}_i, \Omega_i), \tag{15}$$

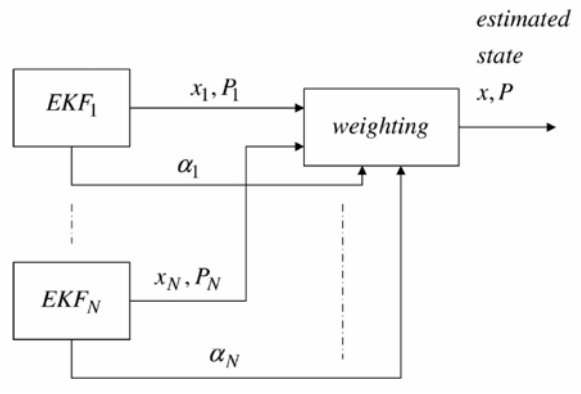

Fig. 2. Concept of Gaussian sum filter.

where N is the number of Gaussians in the sum, α_i is the weight, $\mathbf{m}_i \in \mathbf{R}^d$ and $\Omega_i \in \mathbf{R}^{d\times d}$ are the means and covariances of individual Gaussians

$$\mathbf{N}(\mathbf{m}_i,\Omega_i) = \frac{1}{\sqrt{(2\pi)^d \mid \Omega_i \mid}} \exp(-\frac{1}{2}(\mathbf{x}-\mathbf{m}_i)^T \Omega_i^{-1}(\mathbf{x}-\mathbf{m}_i)), \tag{16}$$

and where d is the dimension of the Gaussian pdf, the weights are constrained by

$$\sum_{i=1}^{N} \alpha_i = 1, \quad \alpha_i \geq 0 \quad \forall i, \tag{17}$$

and the vector of parameters is defined as

$$\vartheta \triangleq [\mathbf{m}_i, \Omega_i] = [m_{i1}, \cdots m_{id}, \Omega_{i1}, \cdots \Omega_{idd}]. \tag{18}$$

When it is required, e.g., to associate measurements to registered landmarks, the aggregated filter output may be calculated sequentially from time k to $k+1$ by

$$\mathbf{x}_{k+1|k+1} = \sum_{i=1}^{N} \alpha_i^{k+1} \mathbf{x}_{i,k+1|k+1}, \tag{19a}$$

$$\mathbf{P}_{k+1|k+1} = \sum_{i=1}^{N} \alpha_i^{k+1} (\mathbf{P}_{i,k+1|k+1} + \bar{\mathbf{P}}_i), \tag{19b}$$

where

$$\begin{aligned} \alpha_i^{k+1} &= \frac{\alpha_i^k \lambda_i}{\sum_{j=1}^{N} \alpha_j^k \lambda_j}, \\ \lambda_i &= \frac{1}{\sqrt{(2\pi)^d \mid \mathbf{S}_i \mid}} \exp(-0.5 \nu_i^T \mathbf{S}_i^{-1} \nu_i), \\ \mathbf{S}_i &= \nabla \mathbf{h} \mathbf{P}_{i,k+1|k} \nabla \mathbf{h}^T + \mathbf{R}, \\ \bar{\mathbf{P}}_i &= (\mathbf{x}_{i,k+1|k+1} - \mathbf{x}_{k+1|k+1})(\mathbf{x}_{i,k+1|k+1} - \mathbf{x}_{k+1|k+1})^T, \end{aligned} \tag{20}$$

and weight α_i^{k+1} is denoted as the normalized weight at time $k+1$, λ_i is the likelihood of an individual EKF, ν_i is the innovation corresponding to meas-urements, $\bar{\mathbf{P}}_i$ is the error covariance matrix and $\mathbf{x}_{i,k+1|k+1}$ is the state estimate from each elementary filter of EKFs.

When the summed representation is applied in the *a priori* pdf in the conditional pdf (3), the stochastic mapping can be carried out by a bank of EKFs as shown in [9]. The remaining problem renders to how to choose the Gaussian sum parameters.

3.1. Choice of parameters

By invoking the principle of maximum entropy for insufficient reasoning, the initial range pdf for a new observed landmark is assigned with a uniform distribution. Assume that a range measurement is available, it is treated as a random variable due to noise corruptions. If one knows the mean and variance, then a Gaussian distribution can be used to describe the measurement without risking over-confidence. If only the mean is available, the exponential distribution is required to represent the variable. On the other hand, when the mean and variance are both unknown, which is the case for a bearing-only sensor, the uniform distribution has to be used instead. In addition, the bearing measurement error distribution can be characterized by a Gaussian distribution as normally found in practical sensors.

Let the bearing sensor operates within a working range, $r \in [r_{min}, r_{max}]$. We assume that the desired pdf is represented by a sum of N Gaussians of a given $p_d(\mathbf{x})$. Now we propose a Gaussian sum with the same number of components as that of the desired pdf, then the probability that the approximation error to be maintained above a threshold can be given by the Chebyshev inequality. That is, for one of the Gaussian

$$P\left(\| \vartheta_p - \vartheta_d \| \geq \varepsilon\right) \leq \frac{\| \Upsilon \|}{\varepsilon^2}, \tag{21}$$

where ϑ_p and ϑ_d are the parameters of the proposed and desired Gaussian sums, ε is the error bound, $\| \Upsilon \|$ is the Frobenius norm [1] for the covariance Υ of the difference between the parameters.

If the N groups of proposal parameters are chosen identically and independently, we may invoke the weak law of large numbers and have

[1] The Frobenius norm, $\| \Upsilon \| = \sqrt{\sum_i \sum_j |\gamma_{ij}|^2}$, is adopted here as the matrix norm because the off-diagonal elements in Υ representing the *orientation* of the distribution are also taken into account.

$$P\left(\| \bar{\vartheta}_p - \vartheta_d \| \geq \varepsilon\right) \leq \frac{\| \Upsilon \|}{N\varepsilon^2} = \tau, \quad (22)$$

where $\bar{\vartheta}_p$ is the sample mean of the parameters, and τ is the error probability threshold.

Examining the above inequality, we see that for a given number of Gaussians and a fixed approximation error ε, the error probability threshold τ is only affected by the distribution of the parameters via Υ. It is, in general, difficult to assign the individual parameters for the proposed Gaussian sum. Alternatively, the choice of parameters should avoid potential risks of being over-confident. Therefore, by invoking the principle of maximum entropy, we maximize the magnitude of the covariance Υ. Since a uniform distribution maintains the largest entropy, we assign the means of the Gaussians to be evenly allocated within the working range $r \in [r_{min}, r_{max}]$. That is

$$m_i = r_{min} + \frac{(r_{max} - r_{min})}{2N}(2i-1), \quad i = 1 \cdots N. \quad (23)$$

Similar argument also leads to the assignment of equal weighting factors when a landmark is firstly initialized, that is

$$\alpha_i = N^{-1}, \quad \forall i. \quad (24)$$

Regarding the selection of the covariances Ω_i, the desired pdf is chosen as uniform over the sensor range. Without loss of generality, assume that the support of the uniform pdf spans ± 1. Furthermore, consider the approximation of this uniform pdf by a single Gaussian (which is normalized to such a scale compatible to the span of the support) as shown in Fig. 3, where the approximation error is shown by the *shaded* areas.

Let the probability of the Gaussian approach zero for the supports far away from ± 1, then the approximation error also tends to zero. Furthermore, let the variance of the Gaussian be selected such that the errors within and beyond the uniform pdf are given by

$$\varepsilon_{in} = \int_{-1}^{1} \left| \frac{1}{\sqrt{2\pi}\sigma} \exp\left(\frac{-x^2}{2\sigma^2}\right) - \frac{1}{2} \right| dx, \quad (25a)$$

$$\varepsilon_{out} = \int_{1}^{\infty} \frac{2}{\sqrt{2\pi}\sigma} \exp\left(\frac{-x^2}{2\sigma^2}\right) dx, \quad (25b)$$

where σ is the variance of the Gaussian.

In addition, let there be a second Gaussian, e.g., on the right-hand side (for positive supports $x > 0$), but the means and variances of the two Gaussians are selected such that they span the same support as

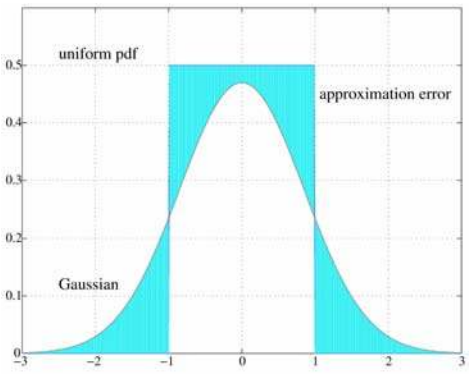

Fig. 3. Gaussian approximation error.

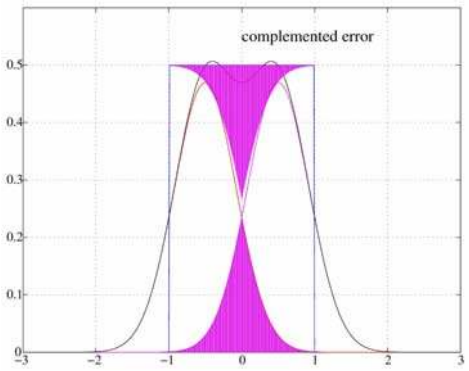

Fig. 4. Complemented approximation error.

before. Then the approximation error from the second Gaussian will complement the first Gaussian, see Fig. 4 (shaded area). Considering the left-hand side Gaussian, the *lack* of representation to the uniform pdf (upper right area) is compensated by the *additive* portion contributed from the second Gaussian on the right-hand side.

Taking the absolute approximation error as a measure of the errors, the exact cancellation of errors within the uniform pdf is achieved by selecting the variance such that the Gaussian function is set at the point where the two Gaussians joint. The variances of the Gaussians can be determined by letting the Gaussian intersect the uniform pdf at $x = 1$ such that the Gaussian is half of its peak, i.e.,

$$\exp\left(\frac{-x^2}{2\sigma^2}\right) = 0.5, \quad (26)$$

or $x = 1.1774\sigma$. Thus

$$\sigma = 0.85, \quad (27)$$

with reference to the ± 1 limits on the uniform pdf. Fig. 5 illustrates the effect of the choice of the Gaussian variance. The graph shows the uniform pdf (rectangle) to be represented and the Gaussians (dotted) and their sum (solid) for the use of 2, 5, 10 and 20 Gaussians respectively. It is observed that a

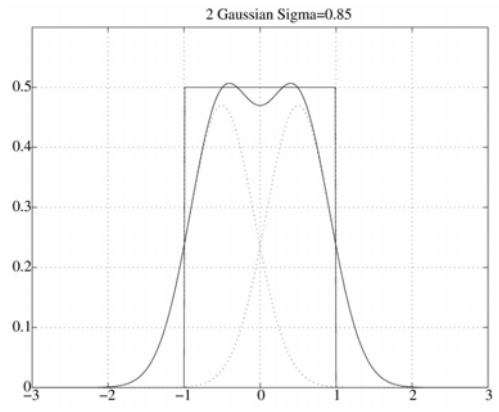

(a)

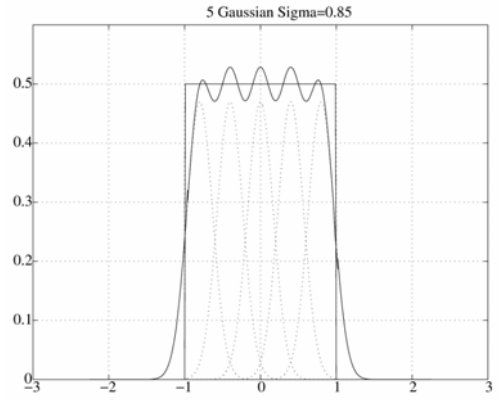

(b)

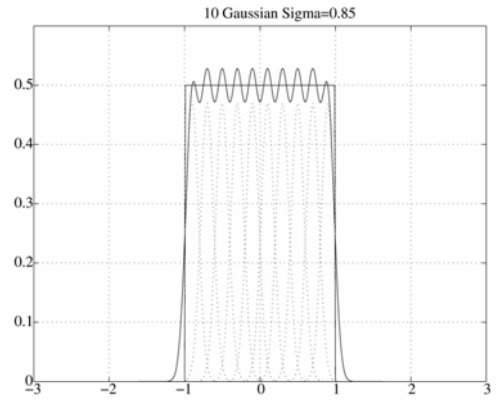

(c)

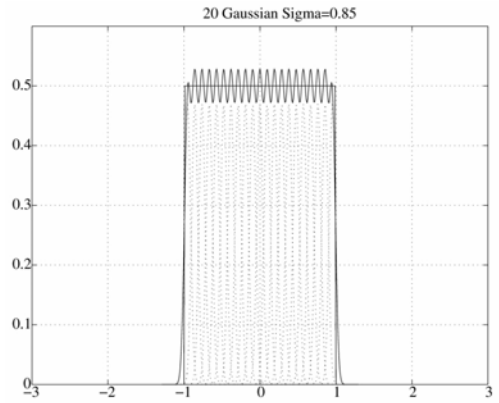

(d)

Fig. 5. Approximation of uniform pdf.

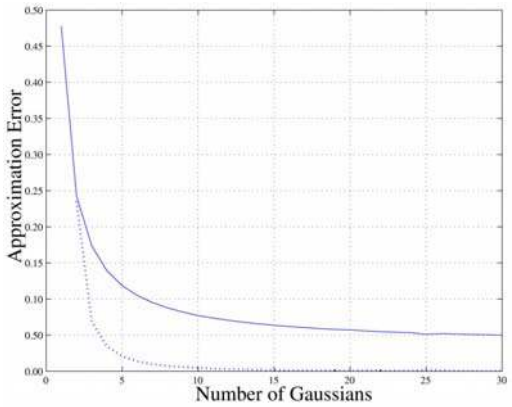

Fig. 6. Approximation error vs. number of Gaussians.

smaller number of Gaussians, e.g., 2 Gaussians, gives a coarse representation; while the use of a larger number of Gaussians (up to 30 Gaussians) provides a very small approximation error.

Note that since the support of the uniform pdf is halved due to the addition of the second Gaussian, the remaining approximation error is also halved. Therefore, the approximation error decreases monotonically when the number of Gaussians increases, provided that the variance of the Gaussians is selected corresponding to the separation of their means, i.e.,

$$\sigma_i = (0.85\Delta m)/2, \quad \forall i, \tag{28a}$$

$$\Delta m = m_{i+1} - m_i, \quad 1 < i < N-1. \tag{28b}$$

Given an error threshold ε, the number of Gaussians can then be calculated. The reduction of the approximation error by adding Gaussians is determined by the number of Gaussians used.

Fig. 6 illustrates the approximation error against the number of Gaussians (solid) and the reduction in the error (dotted). When using more than 8 Gaussians, the reduction in approximation error is not significant as compared to the maximum error from using a single Gaussian. Furthermore, since the approxima-tion error (35, 36) is the integration of the error across the supports, the distribution of the error itself then becomes irrelevant. It is obvious that the law of diminishing return applies in this case, i.e., the gain in using a large number of Gaussians diminishes. Moreover, the number of Gaussians used is also determined by the trade-off between the approxima-tion accuracy and the permissible computational resource. Here, according to the argument stated above, we choose 9 for the number of Gaussians used in the representing the range measurement uncertainty. This number will be reduced, in order to decrease the computational complexity, as described in the following section.

3.2. Reduction of EKFs used

The number of Gaussians or extended Kalman filters used in the Gaussian sum filter, to a certain extent, affects the computational efficiency of the filter. Therefore, the number of EKFs used should be kept as small as possible provided that the range measurement pdf, in the SLAM context, is adequately represented within a specified error limit. The strategy adopted in this work is that when a EKF is ensured of superior performance, the other elementary filters in the GSF are then removed in order to reduce the computational complexity.

3.2.1 Sequential probability ratio test

The sequential probability ratio test (SPRT) is a decision-making technique that allows for the choice of a delayed decision in addition to the conventional acceptance and rejection decisions and does not require a knowledge of the likelihood distribution to derive the decision thresholds.

In our SLAM problem with the Gaussian sum filter approach, the ratio of the innovations from the EKFs is used as the test metric. We define the hypotheses as

$$\begin{aligned} &H_0: \text{this particular EKF truly estimates the system states,} \\ &H_1: \text{any other EKF truly estimates the system states.} \end{aligned} \tag{29}$$

Given the null H_0 and alternative H_1 hypotheses and the thresholds A and B, the test procedure is conducted. At time indexed by k_d, the null hypothesis for the i-th EKF is accepted if

$$\prod_{k=1}^{k_d} \frac{p(\nu_i(k) \mid H_0)}{p(\nu_i(k) \mid H_1)} > A, \tag{30}$$

and the alternative hypothesis is accepted if

$$\prod_{k=1}^{k_d} \frac{p(\nu_i(k) \mid H_0)}{p(\nu_i(k) \mid H_1)} < B, \tag{31}$$

otherwise, additional measurements to obtain $\nu_i(k+1)$ at the next time step are required. Note that $\nu_i(k)$ stands for the innovation of the i-th EKF at time index k.

The relation between the thresholds and decision errors of false alarm α_a and missed detection α_b is given by the following expression and can be user-specified. In our implementation the common practice that both errors are specified at 0.05 is followed.

$$A \approx \frac{1-\alpha_b}{\alpha_a}, \quad B \approx \frac{\alpha_b}{1-\alpha_a}. \tag{32}$$

3.2.2 Test against multiple alternatives

In cases where there are multiple alternatives such as estimates resulting from a bank of EKFs, several choices for the likelihood of the alternative hypothesis may be considered, for example:

Minimum:

$$p(\nu_i \mid H_1) = \min_{j=1, j\neq i} \{p(\nu_j \mid H_1)\}, \tag{33}$$

Maximum:

$$p(\nu_i \mid H_1) = \max_{j=1, j\neq i} \{p(\nu_j \mid H_1)\}, \tag{34}$$

Average:

$$p(\nu_i \mid H_1) = \frac{1}{N-1} \sum_{j=1, j\neq i}^{N} p(\nu_j \mid H_1). \tag{35}$$

The minimum likelihood approach is aggressive, aiming to reduce the number of EKFs in a minimum number of iterations. However, in some situations there may be other equivalently performing EKFs close to the best performing one. At the other end of the spectrum, the maximum ratio strategy adopts a conservative philosophy. It may take extensive filtering iterations before the next high-performing EKF is sufficiently inferior to the best performing EKF. Hence, a delayed improvement on the computational efficiency is expected. The averaging approach smoothes out the likelihood ratio sequences and produces a moderate decision strategy. Thus, it compromises between the risk involved and the efficiency improvement. Therefore, the latter approach is adopted in this work.

3.2.3 Removal of elementary EKFs

Assume that the GSF is operating with a total number of EKFs. When a decision is made according to SPRT, one of the EKFs (e.g., the k-th) will remain in the filter bank (the null hypothesis accepted) while all others are removed from the GSF. The aggregated system estimates (19) are copied to the k-th EKF and its weight is set to unity. The outcome is therefore an efficient implementation of a GSF which reverts to that of using a single EKF, and hence resulting in a significant reduction in complexity.

3.3. Data association and landmark initialization

Data association is the procedure as of how a given measurement is linked to a registered landmark in the system. The conventional approach is used here to implement a nearest neighbor test. Given, for example, a bearing-only measurement θ, its statistic-cal distance to a registered landmark is inferred by the normalization of the difference from the expected bearing, that is

$$\gamma = \nu^2 S^{-1}, \tag{36a}$$

$$\nu = \theta - \hat{\theta}, \tag{36b}$$

$$\hat{\theta} = \arctan\left(\frac{y_f - y_v}{x_f - x_v}\right) - \varphi_v, \tag{36c}$$

$$S = \nabla \mathbf{h}^T \mathbf{P} \nabla \mathbf{h} + \sigma_\theta^2, \tag{36d}$$

where $\hat{\theta}$ is an expected bearing measurement. Note that the innovation and its covariance are calculated corresponding to the aggregated system states.

3.3.1 Associating existed landmarks

When landmarks are observed repeatedly, the measurements will be used to update individual EKFs. Since the measurements are obtained from the real robot and landmarks, data association is conducted using the aggregated state estimations, as given by the procedure of (36). On the contrary, if data association is conducted for an individual EKF, some EKFs will not be updated due to failures in data association. Consequently, the weights of EKFs cannot be adjusted. In this work, we adopt the conventional Mahalanobis distance based nearest-neighbour validation using the χ^2 test. For instance, for a 5% error threshold, the threshold on γ is set at 3.84 for a one degree-of-freedom distribution.

3.3.2 Initializing landmarks

When a new landmark is observed while the GSF is operating, it is incorporated into all the EKFs. Since the location of the new landmark is independent of the landmark estimates in the GSF, it is difficult to assign the weights of individual EKFs after the landmark initialization. The following strategy is adopted on the basis of the fact that, the best estimation at hand is the aggregation of estimations from the EKFs. Here, we regenerate the full number of EKFs by copying the aggregated estimation to all EKFs and initialize each of them using the bearing measurement and a randomly picked pseudo range given by (23). All the weights are reset to N^{-1}.

3.4. Computational complexity

In [5], a particle filter is applied in estimating the ranges of targets using bearing-only sensors. In principle, the PF [6] is a sample-based implementation of the Bayesian estimation theory. Notably, the PF is effective in formulating estimators for non-linear and non-Gaussian systems in contrast to the widely used EKF. The EKF, in turn, is efficient for systems that are linear and uncertainties can be modelled by Gaussian pdfs.

In the PF, a pdf is represented by a large number of particles or samples,

$$p(\mathbf{x}_{PF}) = \sum_{i=1}^{\infty} w_i \delta_i (\mathbf{x} - \mathbf{x}_i), \tag{37}$$

where w_i is the weight of a sample, such that $\sum_i^{\infty} w_i = 1$, and δ_i is a Dirac delta function which is zero everywhere except at $\mathbf{x}_i$.

For the EKF, the pdf is parameterized by its mean $\mathbf{m}$ and variance Ω,

$$p(\mathbf{x}_{KF}) = \frac{1}{\sqrt{(2\pi)^d \,|\Omega|}} \exp\left(-0.5(\mathbf{x} - \mathbf{m})^T \Omega^{-1} (\mathbf{x} - \mathbf{m})\right), \tag{38}$$

where, again, d is the dimension of the Gaussian.

In order to truly approximate an arbitrary pdf, the number of samples used in a PF could approach an intractable large number. Otherwise, if insufficient samples are used (e.g., less than 10000), due to computational resource limitations, sample impoverishment problems [22] may render the PF impracticable. On the other hand, the EKF represents the pdf by parameterizing the mean and variance and the GSF contains a small multiple of these parameters. Therefore, the number of parameters is significantly less than the number of samples used in PFs. The update of the PF also requires to calculate the likelihood functions in accordance to the number of samples. Thus, an additional complexity is further added to the PF implementation.

4. EXPERIMENTS

4.1. Experimental setup and evaluation

Several experiments have been conducted to illustrate the effectiveness of the proposed Gaussian sum filtering approach for mobile robot localization and mapping. The robot, Pionner DX2, is driven to follow several trajectories with different starting positions and in different laboratory environments. The robot moves at 0.15m/sec and turns at ± 6 deg/sec maximum. Furthermore, a laser scanner (SICK LMS200) using only the bearing measurements, as the proof-of-concept, and a camera are used as the sensing device. The laser scanner provides scans across 180° in front of the robot, landmarks are extracted from scans using reflector strips. The camera gives 256 gray-level images of 200×150 pixels resolution, contains a 60° field-of-view, also pointing forward from the robot. Landmarks are extracted from interest points at the transitions of furniture edges and the floor [7].

The estimated robot trajectories resulted from various implementations and the produced maps are used to quantify the effectiveness of the proposed method. Since the range-and-bearing SLAM using a laser scanner has been thoroughly studied, its results are used as the references comparing the results from GSF implementations. In addition, they are also

Compared against a single EKF and the conventional GSF (without EKF reduction by SPRT). The SLAM quantity is evaluated according to the root-mean-squared values of the robot position error as well as the landmark location errors. Moreover, the estimation uncertainties are assessed by the geometric mean between the range-bearing SLAM and the proposed GSF uncertainties. Laser scans of the environment are also included as a visual reference.

4.2. Using bearings from a laser scanner

4.2.1 Trajectory 1

For the test on trajectory 1, Fig. 7, the robot (shown as a triangle) moves on a counterclockwise circular path (the centre circle) where its position is relative to its initial position at time zero. Figs. 7(a) and 7(b) show the mapped environment and the corresponding position error when only odometer feedback is used to estimate the robot position. The map of the environment generated is not satisfactory which shows inconsistence on the laser scans of the laboratory. On the other hand, if the estimated robot position is correct, the laser scans should overlap and produce a concise boundary of the laboratory. The position errors (middle lines in the sub-figures of Fig. 7(b)) also grow unbounded against time (upper and lower lines are the 3σ uncertainty bounds) over the tested period for 500 steps of 0.2sec each due to the accumulation of uncorrected errors.

Results using a single EKF are shown in Figs. 7(c) through 7(e) respectively. The mapped environment shows consistence with the reference range-and-bearing SLAM results. The robot position errors are bounded within the uncertainties and are much reduced as compared to the case of using odometry only. However, it is noted here that the magnitude of uncertainties are larger as compared to the GSF approaches presented in the sequel. Landmark location errors are small but initial errors are larger than the GSF cases, which signified the need for the proper representation of landmark range uncertainty.

A conventional GSF, using 9 EKFs as the proposed GSF, is implemented where the reduction of EKFs is not included. Results are shown in Figs. 7(f) to 7(h). Satisfactory results are depicted for a consistent environment map with small robot and landmark errors. Results from the proposed GSF implementation, with SPRT-based EKF reduction, are depicted in Figs. 7(i) to 7(l). Map and position/ location errors are comparable to the conventional GSF case. In addition, it should be noted here that the number of EKFs included in the GSF, Fig. 7(l), has been reduced to one when the GSF converges with all landmarks in the environment being observed.

4.2.2 Trajectory 2

In this case, the robot is driven in the same laboratory as the previous experiment. However, the robot starts at a different position, thus, a different landmark observation sequence is obtained in this experiment. Results are show in Figs. 8(a) to 8(l) separately. Similar conditions as trajectory 1 are observed in this experiment. Hence, the GSF approach is considered as effective on a different environment and initial condition.

4.2.3 Trajectory 3

The robot is ported to another laboratory and the trajectory starts from a circular path, then a straight line (toward the left-hand side), back to the left and then another semi-circular path. Results are shown in Figs. 9(a) through 9(l). Again, the resultant laboratory map is not satisfactory when using odometry to estimate the robot position. For the rest of the experiments, outcomes are comparable to the previous two cases with the proposed GSF approach producing efficient and effective localization and mapping.

4.2.4 Trajectory 4

A forth trajectory is followed by the robot in the same environment as for trajectory 3, but the robot starts at a different position giving different landmark observation sequences. Figs. 10(a) to 10(l) depict the experimental results obtained in this case. SLAM quantities are equivalent to the previous cases, hence, the proposed approach is also considered satisfactory.

4.3. Using a camera

A camera is further used as the sensor when the robot follows trajectories 1 to 4 respectively. Typical images captured by the camera are shown in Figs. 11 and 12 containing scattered image frames from frame 1 to frame 500 corresponding to the GSF iteration time steps. The scene illustrates test-benches, cabinets and chairs in the laboratory. Furthermore, since laser reflectors are not visually extractable, only robot position errors are considered while landmark errors are not evaluated in the context of localization.

4.3.1 Trajectory 1

Figs. 11(k) and 11(l) contain results for the mapped environment and the robot position errors, respectively. The mapped environment illustrates a consistence as compared to the range-and-bearing SLAM case. The position errors are bounded within the uncertainties. However, due to the limited camera field-of-view and resolution, results are inferior to the experiment using the laser scanner.

4.3.2 Trajectory 2

Results from this experiment are shown in Figs. 11(m) and 11(n). Observations and comments to the results from trajectory 1 also apply here. Moreover, the robot position errors maintain a similar order

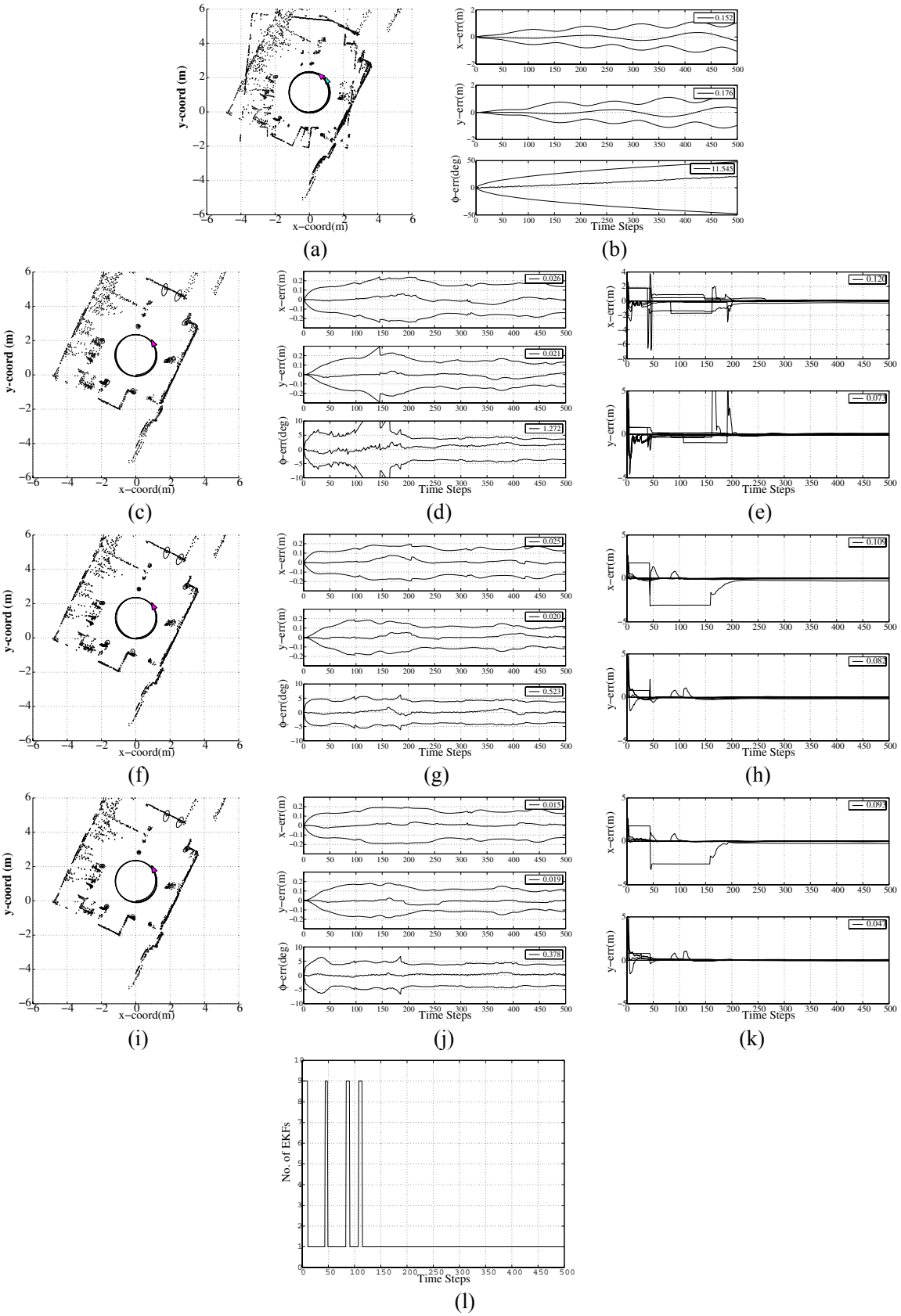

Fig. 7. SLAM results from trajectory 1: Odomoter:- (a) Mapped environment; (b) Robot position error and uncertainty. EKF:- (c) Mapped environment; (d) Robot position error and uncertainties; (e) Landmark errors. Conventional GSF:- (f) Mapped environment; (g) Robot position error and uncertainties; (h) Landmark errors, Proposed GSF:- (i) Mapped environment; (j) Robot position error and uncertainties; (k) Landmark errors; (l) No. of EKFs used in the GSF.

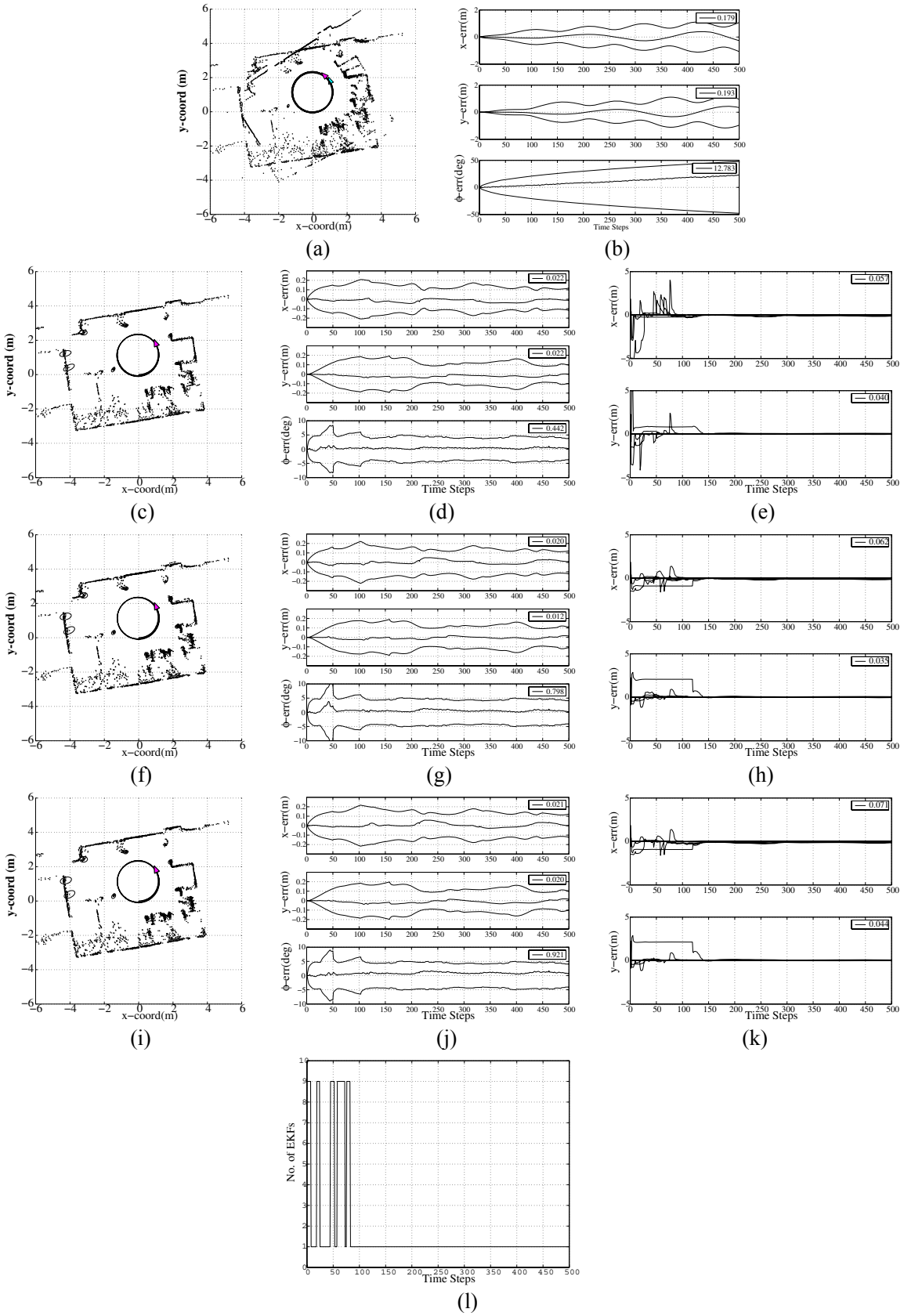

Fig. 8. SLAM results from trajectory 2: Odomoter:- (a) Mapped environment; (b) Robot position error and uncertainty. EKF:- (c) Mapped environment; (d) Robot position error and uncertainties; (e) Landmark errors. Conventional GSF:- (f) Mapped environment; (g) Robot position error and uncertainties; (h) Landmark errors, Proposed GSF:- (i) Mapped environment; (j) Robot position error and uncertainties; (k) Landmark errors; (l) No. of EKFs used in the GSF.

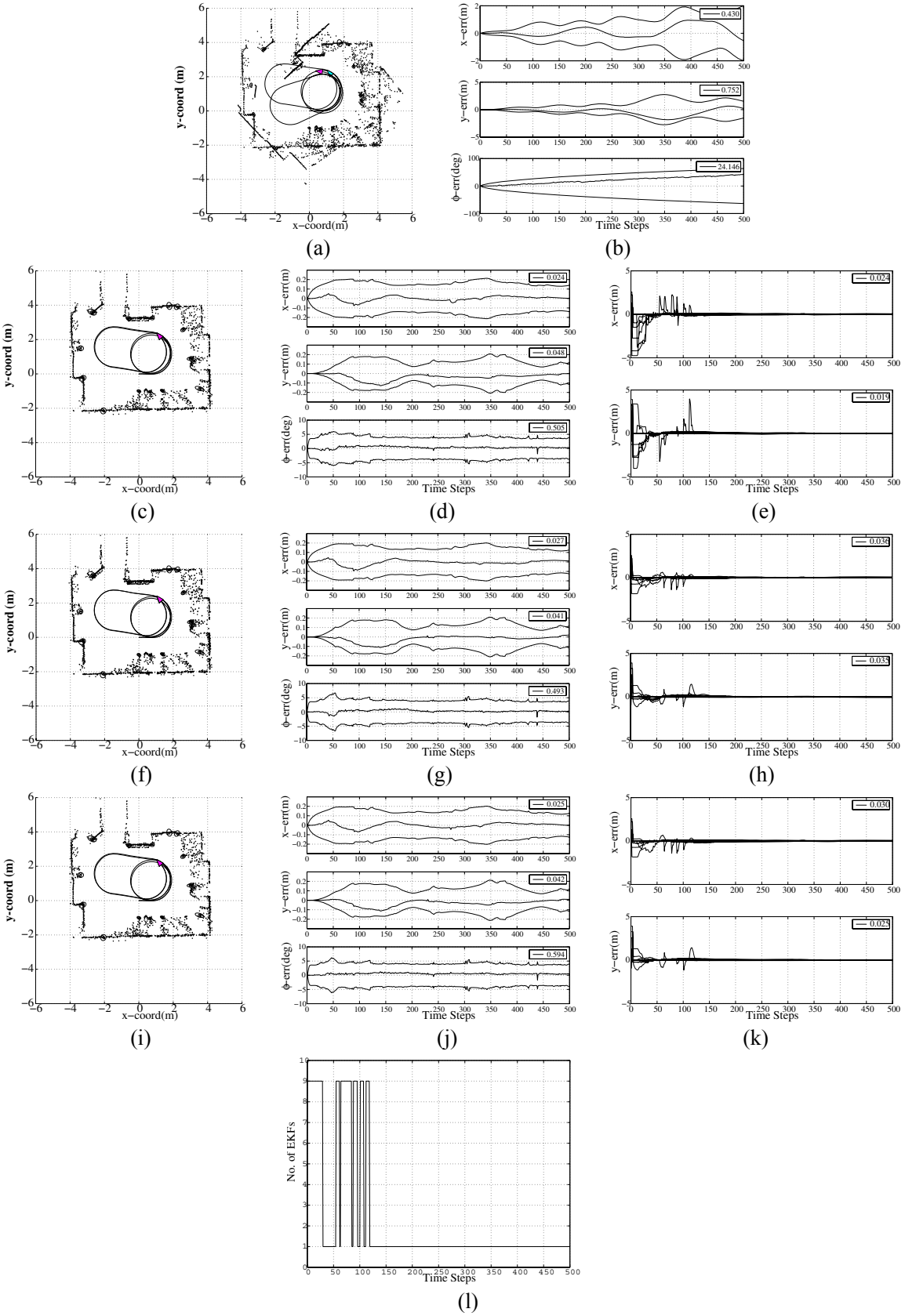

Fig. 9. SLAM results from trajectory 3: Odomoter:- (a) Mapped environment; (b) Robot position error and uncertainty. EKF:- (c) Mapped environment; (d) Robot position error and uncertainties; (e) Landmark errors. Conventional GSF:- (f) Mapped environment; (g) Robot position error and uncertainties; (h) Landmark errors, Proposed GSF:- (i) Mapped environment; (j) Robot position error and uncertainties; (k) Landmark errors; (l) No. of EKFs used in the GSF.

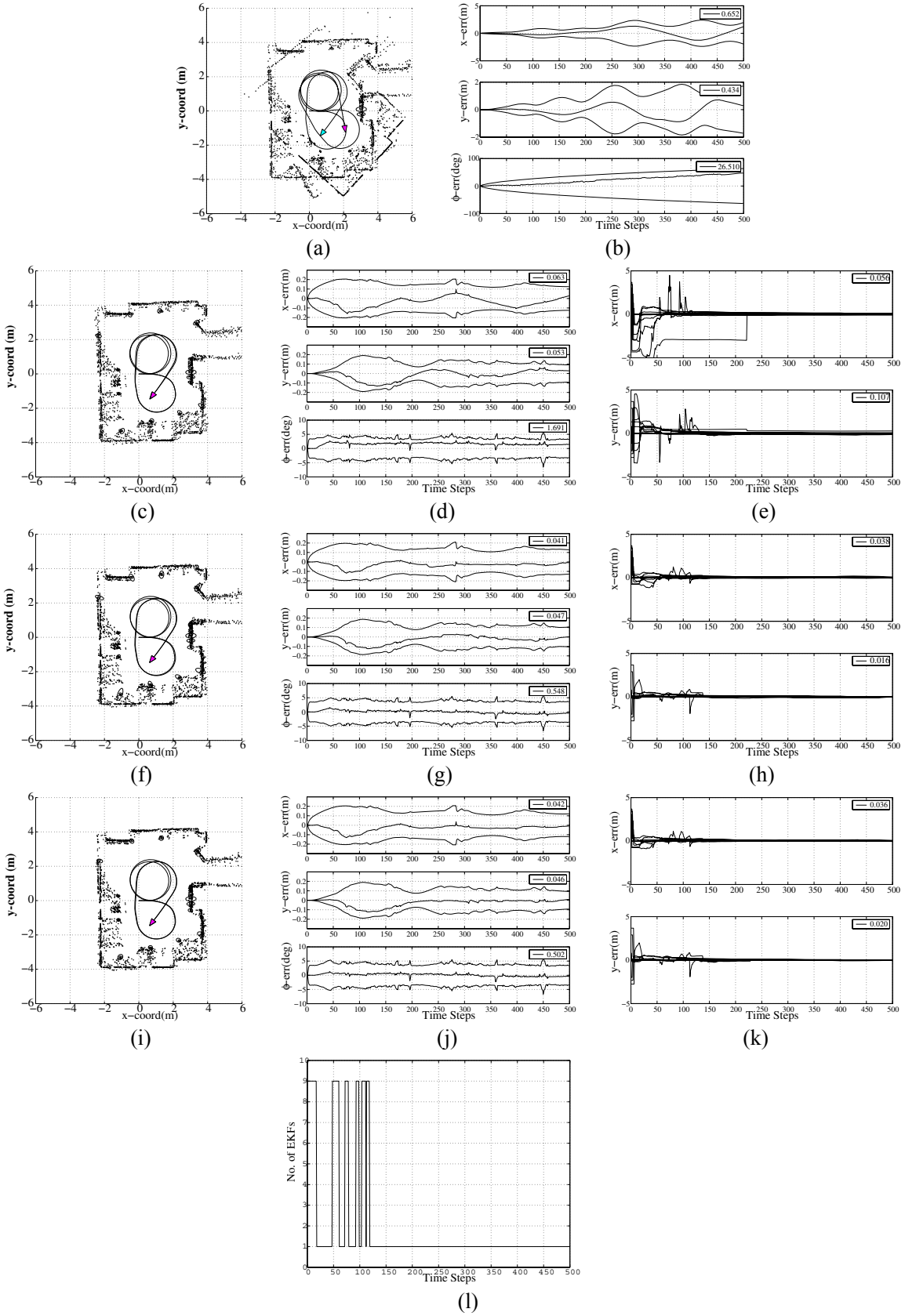

Fig. 10. SLAM results from trajectory 4: Odomoter:- (a) Mapped environment; (b) Robot position error and uncertainty. EKF:- (c) Mapped environment; (d) Robot position error and uncertainties; (e) Landmark errors. Conventional GSF:- (f) Mapped environment; (g) Robot position error and uncertainties; (h) Landmark errors, Proposed GSF:- (i) Mapped environment; (j) Robot position error and uncertainties; (k) Landmark errors; (l) No. of EKFs used in the GSF.

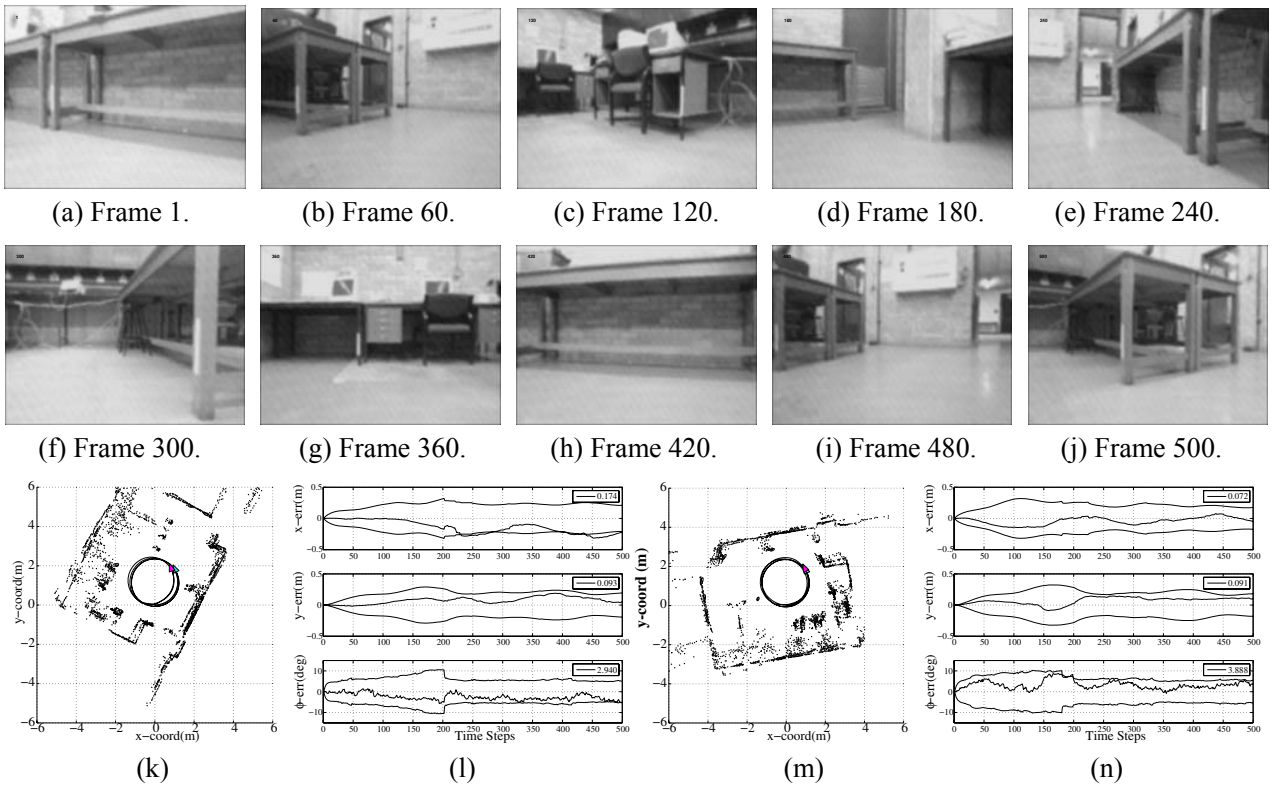

(a) Frame 1. (b) Frame 60. (c) Frame 120. (d) Frame 180. (e) Frame 240.

(f) Frame 300. (g) Frame 360. (h) Frame 420. (i) Frame 480. (j) Frame 500.

(k) (l) (m) (n)

Fig. 11. Typical images of the laboratory environment for trajectories 1 and 2, (a)-(j). SLAM results from using camera: Trajectory 1:- (k) Mapped environment; (l) Robot position error and uncertainty. Trajectory 2:- (m) Mapped environment; (n) Robot position error and uncertainty.

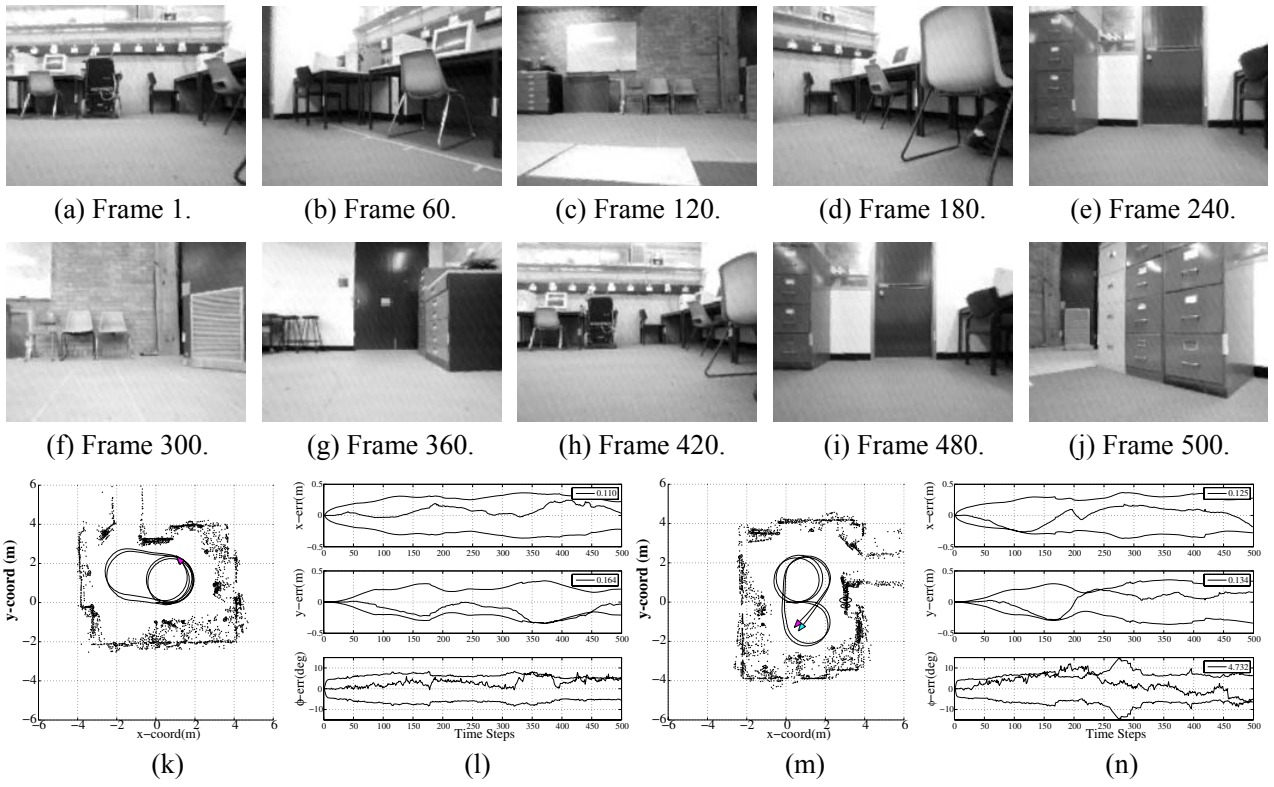

(a) Frame 1. (b) Frame 60. (c) Frame 120. (d) Frame 180. (e) Frame 240.

(f) Frame 300. (g) Frame 360. (h) Frame 420. (i) Frame 480. (j) Frame 500.

(k) (l) (m) (n)

Fig. 12. Typical images of the laboratory environment for trajectories 3 and 4, (a)-(j). SLAM results from using camera: Trajectory 3:- (k) Mapped environment; (l) Robot position error and uncertainty. Trajectory 4:- (m) Mapped environment; (n) Robot position error and uncertainty.

of magnitude as the previous case. Hence, the proposed GSF approach is considered consistent in performance.

4.3.3 Trajectory 3

Figs. 12(k) and 12(l) contain results for the mapped environment and the robot position errors while the robot is following trajectory 3. The mapped environment illustrates, as for trajectories 1 and 2, a consistence as compared to the range-and-bearing SLAM case. The position errors are also bounded within the uncertainties.

4.3.4 Trajectory 4

The robot is further driven in an additional trajectory. Results from this experiment are shown in Figs. 12(m) and 12(n). They are equivalent to the results from trajectory 3 in the previous experiment. However, due to the limited camera field-of-view, occlusion and different landmark observation sequences, results are inferior to those obtained from trajectory 3.

4.4. Discussion

Experimental results are further summarized in Tables 1 and 2. In the tables, the robot position errors are denoted by x_v, y_v, φ_v while the landmark errors are given by f_x, f_y. In Table 1, the first column contains errors resulted from using only the odometry to estimate the robot position. The second column shows errors from using a single EKF for bearing-only SLAM. The third and forth column give results from using a conventional GSF (without EKF reduction) and the proposed GSF (with EKF reduction, and is denoted by SPRT) respectively. These errors are computed by taking the root-mean-squared values over the GSF iteration sequence. The location errors are given in meters (m) and the orientation error is given in degrees ($^\circ$).

In Table 1, the smallest error is indicated in bold-face while the worst ones are denoted in italics. It is observed that the best and worst indicators are spread across the different EKF/GSF implementation approaches. However, it should be emphasized that most worst-case results come from the EKF case while the proposed SPRT implementation gives most of the best results. In addition, worst case errors from the single EKF have a higher order-of-magnitude (shown in bolded-italics) than both the GSF/SPRT approaches. Hence, a single EKF is unreliable in the bearing-only SLAM problem paradigm. It is also further noted that the proposed GSF has used a diminishing number of elementary EKFs in the filter with a reduction in computational complexity.

Results from using a camera are summarized in Table 2. Evidently, errors of equivalent order of magnitudes are observed. Although the orientation errors are larger as anticipated, which is mainly due to limitations in the camera field-of-view and resolution. Nonetheless, the vision-based GSF implementation is performing satisfactorily.

Table 1. Localization and mapping errors: using laser scanner.

Error	Odometry	EKF	GSF	SPRT
Trajectory 1				
x_v	0.152	0.026	0.025	**0.015**
y_v	0.176	0.021	0.020	**0.019**
ϕ_v	11.545	***1.272***	0.523	**0.378**
f_x	NA	0.120	0.109	**0.093**
f_y	NA	0.073	0.082	**0.047**
Trajectory 2				
x_v	0.179	0.022	**0.020**	0.021
y_v	0.193	0.022	**0.012**	0.020
ϕ_v	12.783	**0.442**	0.798	0.921
f_x	NA	**0.057**	0.062	0.071
f_y	NA	0.040	**0.035**	0.044
Trajectory 3				
x_v	0.430	**0.024**	0.027	0.025
y_v	0.752	0.048	**0.041**	0.042
ϕ_v	24.146	0.505	**0.493**	0.594
f_x	NA	**0.024**	0.036	0.030
f_y	NA	**0.019**	0.035	0.025
Trajectory 4				
x_v	0.652	0.063	**0.041**	0.042
y_v	0.434	0.053	0.047	**0.046**
ϕ_v	26.510	***1.691***	0.548	**0.502**
f_x	NA	0.056	0.038	**0.036**
f_y	NA	0.107	**0.016**	0.020

Table 2. Localization errors: using camera.

Trajectory	Error		
	x_v	y_v	ϕ_v
1	0.174	0.093	2.940
2	0.072	0.091	3.888
3	0.110	0.164	3.566
4	0.125	0.134	4.732

5. CONCLUSIONS

We have presented a Gaussian sum filter for the estimation of the mobile robot pose and landmark

locations, in the SLAM context for an unstructured environment using a bearing-only sensor. Due to the lack of range measurements, stochastic mapping using an EKF is replaced with a Gaussian sum filter in the form of a bank of EKFs. The parameters of the initial Gaussians are determined on the basis of the approximation error incurred by using the Gaussian sum for representing a uniform probability density function. A proper compromise between the accuracy and complexity suggests a practically tractable initial number of EKFs to be used. The implementation complexity is further reduced by removing non-performing EKFs via the sequential probability ratio test. The ultimate GSF then reverts to a single EKF. Experiments have been conducted using the bearing measurements form a laser scanner and a camera as the bearing-only sensors in several environments and trajectories followed by the robot. Our results have shown that the proposed GSF implementation method is effective and efficient. Further work is directed towards implementations in large operating environments.

REFERENCES

[1] S. Thrun, "Robotic mapping: A survey," *Technical Report, CMU-CS-02-111*, School of Comp. Sci., Carnegie Mellon University, 2002.

[2] R. Smith, M. Self, and P. Cheesman, "Estimating uncertain spatial relationships in robotics," *Intl. Journal of Autonomous Robot Vehicles*, pp. 167-193, 1990.

[3] R. J. Rikoski, J. J. Leonard, and P. M. Newman, "Stochastic mapping frameworks," *Proc. of IEEE Intl. Conf. on Robotics and Automation*, Washington, DC, pp. 426-433, May 2002.

[4] G. Dissanayake, P. Newman, S. Clark, H. F. Durrant-Whyte, and M. Csobra "A solution to the simultaneous localization and mapping (SLAM) problem," *IEEE Trans. on Robotics and Automation*, vol. 17, no. 3, pp. 229-241, June 2001.

[5] R. Karlsson and F. Gustafsson, "Range estimation using angle-only target tracking with particle filters," *Proc. of American Control Conference*, Arlington, VA, pp. 3743-3748, June 2001.

[6] N. J. Gordon, D. J. Salmond, and A. F. M. Smith, "Novel approach to nonlinear/non-Gaussian Bayesian state estimation," *IEE Proceedings-F*, vol. 140, no. 2, pp. 107-113, April 1993.

[7] N. M. Kwok and A. B. Rad, "A modified particle filter for simultaneous localization and mapping," *Journal of Intelligent and Robotic Systems*, vol. 46, no. 4, pp. 365-382, 2006.

[8] R. Chen and J. S. Liu, "Mixture Kalman filters," *Journal of Royal Statistical Society B*, vol. 62, Part 3, pp.493-508, 2000.

[9] D. L. Alspach, "A Gaussian sum approach to the multi-target identification-tracking problem," *Automatica*, vol. 11, pp. 285-296, 1975.

[10] W. S. Chaer, R. H. Bishop, and J. Ghosh, "A mixture-of-experts framework for adaptive Kalman filtering," *IEEE Trans. on System, Man and Cybernetics-Part B: Cybernetics*, vol. 27, no. 3, pp. 452-464, June 1997.

[11] W. I. Tam, K. N. Plataniotis, and D. Hatzinakos, "An adaptive Gaussian sum algorithm for radar tracking," *Signal Processing*, vol. 77, pp. 85-104, 1999.

[12] Y. S. Kim and K. S. Hong, "An IMM algorithm for tracking maneuvering vehicles in an adaptive cruise control environment," *International Journal of Control, Automation and Systems*, vol. 2, no. 3, pp. 310-318, September 2004.

[13] X. R. Li and Y. Bar-Shalom, "Design of an interacting multiple model algorithm for air traffic control tracking," *IEEE Trans. on Control Systems Technology*, vol. 1, no. 3, pp. 186-194, September 1993.

[14] T. Bailey, "Constrained initialization for bearing-only SLAM," *Proc. of IEEE Intl. Conf. on Robotics and Automation*, Taipei, Taiwan, pp. 1966-1971, September 2003.

[15] A. Costa, G. Kantor, and H. Choset, "Bearing-only landmark initialization with unknown data association," *Proc. of IEEE Intl. Conf. on Robotics and Automation*, New Orleans, LA, pp. 1764-1770, April/May 2004.

[16] N. M. Kwok, G. Dissanayake, and Q. P. Ha, "Bearing-only SLAM using a SPRT based Gaussian sum filter," *Proc. of IEEE Intl. Conf. on Robotics and Automation*, Barcelona, Spain, pp. 1121-1126, April 2005.

[17] J. Sola, A. Monin, M. Devy, and T. Lemaire, "Undelayed initialization in bearing only SLAM," *Proc. of IEEE/RSJ Intl. Conf. on Intelligent Robots and Systems*, Edmonton, Canada, pp. 2751-2756, August 2005.

[18] T. R. Kronhamn, "Bearings-only target motion analysis based on a multihypothesis Kalman filter and adaptive ownship motion control," *IEE Proc.-Radar, Sonar and Navigation*, vol. 145, no. 4, pp. 247-252, August 1998.

[19] N. Vlassis and A. Likas, "A greddy EM algorithm for Gaussian mixture learning," *Neural Processing Letters*, vol. 15, no. 1, pp. 77-87, 2002.

[20] J. L. Williams and P. S. Mayback, "Cost-function-based Gaussian mixture reduction for target tracking," *Proc. of the 6th Intl. Conf. on Information Fusion*, Cairns, Australia, pp. 1047-1054, July 2003.

[21] X. Q. Li and I. King, "Gaussian mixture distance for information retrieval," *Proc. of Intl. Joint*

Conf. on Neural Networks, Washington, DC, pp. 2544-2549, July 1999.

[22] N. M. Kwok, G. Fang, and W. Zhou, "Evolutionary particle filter: re-sampling from the genetic algorithm perspective," *Proc. of IEEE/RSJ Intl. Conf. Intelligent Robots and Systems*, Edmonton, Canada, pp. 1053-1058, August 2005.

Ngai Ming Kwok obtained the B.Sc. degree in Computer Science from the University of East Asia, Macau, P. R. China, the M.Phil. degree in Control Engineering from The Hong Kong Polytechnic University, P. R. China and has completed the Ph.D. degree in Mobile Robotics from the University of Technology, Sydney, Australia in 1993, 1997 and 2006 respectively. He is currently a Senior Research Assistant at the Faculty of Engineering, University of Technology, Sydney, Australia. His research interests include mobile robotics, evolutionary computing and intelligent control.

Quang Phuc Ha received the B.E. degree in Electrical Engineering from Ho Chi Minh City University of Technology, Vietnam, the Ph.D. degree in Engineering Science from Moscow Power Engineering Institute, Russia, and the Ph.D. degree in Electrical Engineering from the University of Tasmania, Australia, in 1983, 1992, and 1997, respectively. He is currently an Associate Professor at the Faculty of Engineering, University of Technology, Sydney, Australia. His research interests include robust control and estimation, robotics, and applications of artificial intelligence.

Shoudong Huang received his Bachelor and Master degrees in Mathematics, and his Ph.D. in Automatic Control from Northeastern University, P. R. China in 1987, 1990, and 1998, respectively. He had been with the Northeastern University, P. R. China, The Hong Kong University, P. R. China and The Australian National University, Australia. He is currently a Lecturer in the Faculty of Engineering, University of Technology, Sydney, Australia. His research interests include nonlinear systems control and mobile robot localization and mapping.

Gamini Dissanayake is the James N. Kirby Professor of Mechanical and Mechatronic Engineering at the University of Technology, Sydney (UTS), Australia. He graduated in Mechanical/Production Engineering from the University of Peradeniya, Sri Lanka. He received his M.Sc. in Machine Tool Technology and Ph.D. in Mechanical Engineering (Robotics) from the University of Birmingham, England in 1981 and 1985 respectively. He currently leads the UTS node of the Australian Research Council Centre of Excellence for Autonomous Systems. His research interests are in the areas of localization and map building for mobile robots, navigation systems, dynamics and control of mechanical systems, cargo handling, optimization and path planning.

Gu Fang received a B.Eng. degree in Mechanical Automation from Shanghai University of Technology in China, and a Ph.D. degree from the University of Sydney in Australia. Since 1996 he has worked as a Lecturer then a Senior Lecturer in the School of Engineering at the University of Western Sydney, Australia. He is also a Visiting Scholar at the ARC Centre of Excellence for Autonomous Systems at the University of Technology, Sydney, Australia. His main research interests include mobile robot exploration and control, neural network and fuzzy logic control in robotics, force control for industrial robots and robot applications in healthcare and construction.